Preprints of the 23rd IFAC World Congress
Busan, Republic of Korea, August 23-28, 2026

Barrier-Certified Multi-Agent Ergodic Coverage over Complex Surfaces

Ali Aminzadeh * **Azwirman Gusrialdi** *

* *Faculty of Engineering and Natural Sciences, Tampere University, Finland (e-mail: ali.aminzadeh@tuni.fi, azwirman.gusrialdi@tuni.fi).*

Abstract: This paper presents a barrier-certified multi-agent ergodic coverage framework for safe and efficient exploration over complex non-Euclidean surfaces. We address the challenge of extending surface ergodic exploration to distributed multi-agent systems (MASs), where globally coupled ergodic statistics must be estimated cooperatively while satisfying safety and communication constraints. Building on the Laplace–Beltrami (LB) eigenbasis, we formulate a distributed ergodic coverage problem on meshable surfaces that enables cooperative exploration with respect to a desired inspection density. Safety is enforced through a unified set of control barrier functions (CBFs) guaranteeing inter-agent collision avoidance, distance-based connectivity, line-of-sight (LOS) preservation, and minimum surface clearance, leading to geometry-dependent couplings. A distributed consensus mechanism enables cooperative estimation of global ergodic statistics without centralized coordination, while maintaining performance and improving scalability. The framework is validated in a simulated 3D wind turbine inspection scenario.

Keywords: Ergodic search, meshable surfaces, control barrier function, safe multi-agent systems, connectivity maintenance

1. INTRODUCTION

The autonomous inspection of large-scale complex 3D structures and surfaces has emerged as a critical capability in modern infrastructure systems, with applications ranging from wind turbines and offshore platforms to bridges, dams, and industrial facilities. These tasks require efficient and reliable coverage strategies over complex surfaces while ensuring safe operation in challenging environments. Manual approaches are slow, hazardous, and costly, often requiring prolonged system shutdowns during inspection. For example, in offshore wind turbine inspection, downtime can account for up to 25–30% of total lifetime costs (Rinaldi et al., 2021). While autonomous single-robot inspection systems offer a promising solution to reduce costs and enhance operational reliability, they remain limited by battery life, wind constraints, and restricted sensing coverage, reducing operational efficiency and scalability.

In contrast, multi-agent systems (MASs) enable cooperative inspection, significantly increasing coverage speed and robustness (Aminzadeh and Khoshnood, 2023) while reducing downtime. Coordinated MASs support task distribution, persistent operation, and redundancy, making them well suited for large-scale wind farm inspection, where coverage control ensures inspection of critical areas while minimizing redundancy and optimizing energy use. Prior knowledge of likely defect locations can be encoded as a spatial probability distribution, naturally fitting the *ergodic search* framework, which allocates exploration effort proportionally.

⋆ This work was supported in part by the Research Council of Finland under the Profiling Action on System-on-Chip and Wireless Technology for Intelligent Machines at Tampere University.

Traditional ergodic search methods (Miller and Murphey, 2013; Mathew and Mezić, 2011), however, are limited to simple domains (e.g., Euclidean planes or spheres) with analytical Fourier bases. Despite their appeal, the ergodic metric scales exponentially with dimension (Shetty et al., 2021), restricting applicability to low-dimensional (< 3D) spaces (Ivić et al., 2023). Many vision and manipulation tasks occur in complex non-Euclidean environments. To address this, we build on (Dong et al., 2025), extending ergodic search via trajectory optimization and Laplace–Beltrami (LB) eigenfunctions to arbitrary 3D manifolds, and further generalize it to MASs for coordinated exploration over complex surfaces.

Beyond coverage efficiency, ensuring safe operation—i.e., avoiding unsafe regions—remains challenging in complex, cluttered, and dynamic environments. Existing ergodic coverage methods often lack provable safety guarantees. Motivated by this, we develop an approach for MASs that integrates ergodic exploration with formal safety guarantees. To achieve this, we employ Lyapunov-like barrier functions, known as *control barrier functions* (CBFs) (Borrmann et al., 2015), which ensure trajectories remain within invariant safe sets and are well-suited for coordinated MASs. CBFs have gained traction for scalable, safety-critical controller synthesis (Ames et al., 2019).

Original Contributions. This paper makes the following contributions: (i) We formulate a MAS ergodic exploration framework over meshable manifolds, extending LB-based ergodic metrics to distributed MAS settings. Unlike Euclidean approaches based on Fourier bases, which allow local evaluation, LB eigenfunctions depend on the entire mesh and must be computed globally. Consequently, agents cannot evaluate ergodic statistics using

©2026 the authors. Accepted by IFAC for publication under a Creative Commons Licence CC-BY-NC-ND

only local information, making distributed implementation significantly more challenging. (ii) To address this challenge, we decompose the ergodic statistics into local contributions and introduce a distributed consensus-based scheme that enables each agent to estimate the global ergodic coefficients through local communication, eliminating the need for centralized computation. (iii) We develop a unified CBF framework that jointly enforces collision avoidance, distance-based connectivity, line-of-sight (LOS) preservation, and surface clearance on complex geometries, where these constraints become nonlinear and geometry-dependent. (iv) We integrate ergodic exploration and safety-critical control into a distributed optimization framework, enabling coordinated and provably safe MAS coverage over non-Euclidean domains.

Related Literature and Research Gaps. To the best of our knowledge, no prior work addresses safety-integrated multi-agent ergodic search over such surfaces. Our approach builds on (Dong et al., 2025), which is limited to single-agent systems and does not consider connectivity or formal safety guarantees. While (Lerch et al., 2023) proposes safety-critical ergodic search for MASs, it is restricted to Euclidean domains, lacks connectivity maintenance, and relies on centralized computation, limiting scalability. Similarly, (Yang et al., 2024) considers LOS connectivity but does not address ergodic search or integrate formal safety guarantees. In contrast, we formulate an optimization-based ergodic search framework over complex surfaces that jointly enforces collision avoidance, connectivity maintenance, and LOS preservation. Although (Ivić et al., 2023) studies multi-agent ergodic search on complex surfaces, it requires solving a PDE dependent on the information map, which must be recomputed when the map changes and may yield poor performance for short trajectories. Moreover, it does not account for connectivity, LOS preservation, or formal safety guarantees, considering only a fixed safe distance from the structure. Finally, our method is limited to position-based ergodic coverage. In contrast, (Sun et al., 2025) introduces orientation-aware ergodic coverage, but it is restricted to single-agent systems and does not incorporate safety or connectivity, which are essential for reliable multi-agent operation in complex environments.

2. PROBLEM FORMULATION

2.1 Preliminaries

Let us consider a MAS consisting of N agents indexed by $i \in \{1, \dots, N\}$. The continuous-time dynamics of agent i is given by $\dot{x}_i = \mathscr{F}_i(x_i, u_i)$, where $x_i \in X_i \subset \mathbb{R}^{n_i}$ denotes the state of agent i, $u_i \in U_i \subset \mathbb{R}^{m_i}$ its control input, and $\mathscr{F}_i : X_i \times U_i \to X_i$ represents the agent dynamics, assumed to be continuous and differentiable. Assuming a homogeneous set of agents, we stack the individual states and define the overall system state as $x = [x_1, x_2, \dots, x_N] \in X \subset \mathbb{R}^n$, $n = \sum_{i=1}^N n_i$. Similarly, the stacked control input is defined as $u = [u_1; \dots; u_N] \in U \subset \mathbb{R}^m$, $m = \sum_{i=1}^N m_i$, where $X := \prod_{i=1}^N X_i$ and $U := \prod_{i=1}^N U_i$. The continuous-time dynamics of the MAS consisting of N agents is given by $\dot{x} = \mathscr{F}(x, u)$, where $\mathscr{F}(x, u) = [\mathscr{F}_1(x_1, u_1); \dots; \mathscr{F}_N(x_N, u_N)]$.

2.2 Spanning-Tree

Let $\mathcal{G} = (V, E)$ be an undirected graph, where $V := \{1, \dots, N\}$ is the set of nodes, and $E \subseteq V \times V$ is the set of edges or communication links between nodes. An edge $(i, j) \in E$ denotes that node j can receive information from node i. Since the graph $\mathcal{G}$ is undirected, we have $(i, j) \in E \Leftrightarrow (j, i) \in E$. The graph $\mathcal{G}$ is connected if and only if every pair of nodes in V is linked by a path. A tree is a connected acyclic graph. A spanning tree of $\mathcal{G}$ is a subgraph $\mathcal{G}_\mathcal{T} = (V, E_\mathcal{T})$ with $E_\mathcal{T} \subseteq E$ that contains all vertices and forms a tree. A path graph is a special spanning tree whose maximum node degree is two, corresponding to a line topology. Hence, a spanning tree is a connected, acyclic subgraph satisfying $|E_\mathcal{T}| = N - 1$ and $E_\mathcal{T} \subseteq E$.

In the following subsection, we provide formal safety guarantees following (Egerstedt, 2021).

2.3 Control Barrier Functions (CBFs)

To ensure the safety (satisfying) of specifications between agents (e.g., collision avoidance, connectivity maintenance, etc.), we consider a *pairwise safe set* between agents i and j ($i \neq j$) defined as

$$\mathcal{S}_{ij} = \{(x_i, x_j) \in X_i \times X_j \mid h_{ij}(x_i, x_j) \geq 0\}, \tag{1}$$

where $h_{ij} : X_i \times X_j \to \mathbb{R}$ is a continuously differentiable function encoding the safety constraint between agents i and j. The pairwise safe set $\mathcal{S}_{ij}$ is forward invariant if

$$\begin{aligned} \dot{h}_{ij}(x_i, x_j) &= \nabla_{x_i} h_{ij}(x_i, x_j) \cdot \mathscr{F}_i(x_i, u_i) \\ &+ \nabla_{x_j} h_{ij}(x_i, x_j) \cdot \mathscr{F}_j(x_j, u_j) \geq -\gamma_{ij}(h_{ij}(x_i, x_j)), \end{aligned} \tag{2}$$

for some class-$\mathcal{K}_\infty$ function γ_{ij} and with $\nabla_{x_i} h_{ij} \neq 0$, $\nabla_{x_j} h_{ij} \neq 0$. In this case, h_{ij} is called a pairwise *control barrier function* (CBF). The dot "$\cdot$" denotes the inner product, and $\nabla_{x_i} h_{ij}$ (resp. $\nabla_{x_j} h_{ij}$) is the gradient of h_{ij} with respect to x_i (resp. x_j).

We now recall the following lemma from (Ibuki et al., 2023, Thm. 4.1), which states that if condition (2) holds for each (i, j) pair, then any trajectory of agents i and j starting in $\mathcal{S}_{ij}$ will remain in $\mathcal{S}_{ij}$ for all future time.

Lemma 1. *Consider a pair of agents i and j with states denoted by x_i and x_j, respectively. Suppose a pairwise CBF $h(x_i, x_j)$ satisfies $h(x_i, x_j) = h(x_j, x_i)$ and $\nabla_{x_j} h_{ij}(x_i, x_j) \neq 0$. Then any Lipschitz continuous controllers u_i and u_j satisfying* (2) *render the pairwise safe set* (1) *forward invariant.*

2.4 Multi-Agent Fourier Ergodic Search

Let W be the exploration domain. The spaces X and W are linked by a sensor model $\mathbb{S}^x(w) : X \times W \to \mathbb{R}$, which describes the information density collected at $w \in W$ when the MAS is at state $x \in X$. The sensor model satisfies $\mathbb{S}^x(w) > 0$ and need not be normalized, capturing how well the MAS observes each point in W. In classical ergodic search, $\mathbb{S}^x$ is a Dirac delta function δ^x, meaning the agent observes only its current location. Given the MAS trajectory $x(\cdot)$, we define the unnormalized time-averaged statistics $\bar{\mu}^{x(\cdot)}(w) = \frac{1}{t_f} \int_0^{t_f} \mathbb{S}^{x(t)}(w) dt$ as a measure of the information gathered at each point in W. The normalized distribution $\mu^{x(\cdot)}(w) = \frac{\bar{\mu}^{x(\cdot)}(w)}{\int_W \bar{\mu}^{x(\cdot)}(w) dw}$ is then obtained by normalizing over W.

In the infinite time limit $t_f \to \infty$, a trajectory $x(t)$ is ergodic over W if its time-averaged information $\mu^{x(\cdot)}(w)$ converges weakly to the target distribution $\phi : W \to \mathbb{R}^+$. The function $\phi(w)$, known as the *information map*, is typically derived from expected information density (Miller et al., 2015; Mavrommati et al., 2017). This implies that the trajectory allocates search effort proportionally to ϕ. Formally, ergodicity holds if, for all Lebesgue functions $\mathcal{F} \in \mathcal{L}^1$ (Scott et al., 2009), $\lim_{t_f\to\infty} \int_W \mathcal{F}(w)\, \mu^{x(\cdot)}(w)\, dw = \int_W \mathcal{F}(w)\, \phi(w)\, dw$.

The goal of multi-agent coverage is to drive the MAS state $x(t) = [x_1(t); \ldots; x_N(t)]$ so that the trajectory statistics $\mu^{x(\cdot)}(w)$ match the information map $\phi(w)$ under an ergodic metric. In finite time, exact matching is not expected; instead, the mismatch is quantified by a weighted squared norm between $\mu^{x(\cdot)}(w)$ and $\phi(w)$ in a spectral domain. In the optimization problem (3), μ_s and ϕ_s are the s-th basis coefficients of the $\mu^{x(\cdot)}$ and ϕ distributions, respectively, computed using the basis functions $\mathcal{F}_s$.

$$\begin{aligned} \min_{x,u} \quad & \mathcal{E}(x(t),\phi) = \sum_{s=0\in\mathbb{Z}^n}^{S\in\mathbb{Z}^n} \Lambda_s \left(\mu_s - \phi_s\right)^2 \\ \text{s.t.} \quad & \dot{x}_i(t) = \mathscr{F}(x_i(t), u_i(t)), \quad \forall i \in V := \{1,\ldots,N\}, \\ & x_i(t) \in X_i,\ u_i(t) \in U_i, \quad \forall i \in V := \{1,\ldots,N\}, \end{aligned} \tag{3}$$

with coefficients defined as

$$\mu_s = \int_W \mathcal{F}_s(w) \mu^{x(\cdot)}(w)\, dw \tag{4}$$

$$\phi_s = \int_W \mathcal{F}_s(w) \phi(w)\, dw \tag{5}$$

Here, $S \in \mathbb{Z}^n$, and s is a multi-index, $s = (s_1, s_2, \ldots, s_n)$. Following (Mathew and Mezić, 2011), the weighting term is defined as $\Lambda_s = \frac{1}{\left(1+\|s\|^2\right)^l}$, $l = \frac{n+1}{2}$. For hypercube W, the basis functions coincide with the Fourier basis:

$$\mathcal{F}_s(w) = \frac{1}{h_s} \prod_{p=1}^{n} \cos\left(\frac{w_p s_p \pi}{L_p}\right), \tag{6}$$

where h_s is a normalization factor (Miller et al., 2015), and L_p, $p = 1, \ldots, n$, denotes the hyper-rectangular domain length along dimension p.

While prior MAS ergodic search works typically consider Euclidean domains (e.g., hypercubes) (Lerch et al., 2023; Kosonen et al., 2025), following Dong et al. (2025), We generalize to arbitrary manifolds in $\mathbb{R}^n$.

2.5 Multi-Agent Surface Ergodic Exploration

Approximation of Basis Functions. The main challenge in extending the Fourier ergodic metric to manifolds is selecting basis functions on W that form an orthonormal set, $\int_W \mathcal{F}_s \mathcal{F}_{s'}\, dw = \delta_{ss'}$, where $\delta_{ss'}$ denotes the Kronecker delta, enabling efficient computation of μ_s and ϕ_s, while also permitting higher-order terms to be discounted via Λ_s to ensure convergence of Eq. (3) as $S \to \infty$, thereby motivating frequency-related properties. While Fourier basis functions (Eq. (6)) satisfy these in Euclidean domains, they are not orthonormal on arbitrary manifolds W; thus, following (Dong et al., 2025), we generalize them using the LB operator Δ, whose eigenfunctions (Eq. (7)) are orthonormal due to its Hermitian property, with eigenvalues corresponding to frequency (Sharp and Crane, 2020).

$$\Delta \mathcal{F}_s = \lambda_s \mathcal{F}_s \tag{7}$$

In Euclidean space, the eigenfunctions of Δ coincide with Fourier bases, making the approach of (Dong et al., 2025) consistent with prior methods. In practice, Δ is approximated by a discretized LB operator $\mathbb{L}$ on a simplicial manifold $\mathscr{M}$ that approximates W; in $\mathbb{R}^3$, $\mathscr{M}$ is a triangular mesh, and W is restricted to admit mesh sequences converging in Hausdorff distance and area and forming normal graphs (Hildebrandt et al., 2006), ensuring $\mathbb{L} \to \Delta$ in operator norm. For a triangle mesh with m vertices, $\mathbb{L}$ is an $m \times m$ matrix (Sharp and Crane, 2020), and functions $\mathcal{F} : W \to \mathbb{R}$ are approximated on $\mathscr{M}$ as length-m vectors via area elements $E_b \subset \mathscr{M}$ at vertices v_b: $\boldsymbol{\mathcal{F}} = \left[\int_{E_b} \mathcal{F}(v)\, dv \approx \mathcal{F}(v_b)\mathrm{Area}(E_b)\right]_{b=1}^{m}$. This yields the matrix eigenvalue problem analogous to (7):

$$\mathbb{L}\boldsymbol{\mathcal{F}}_s = \lambda_s \boldsymbol{\mathcal{F}}_s \tag{8}$$

It is shown in Dong et al. (2025) that as the mesh $\mathscr{M}$ converges to W, the ergodic metric computed on $\mathscr{M}$ using the eigenvectors from Eq. (8) converges to the metric defined on W using the eigenfunctions from Eq. (7). We adopt the following corollary and theorem from this work; see the same reference for proofs.

Corollary 1. *Let the ergodic discounting factor $\Lambda_s = \eta(\lambda_s)$ be a power series. Then the ergodic metric calculated using the continuous LB operator Δ is $\mathcal{E}^{\Delta} = \langle \phi - \mu^{x(\cdot)}, \eta(\Delta)(\phi - \mu^{x(\cdot)})\rangle$ and the ergodic metric calculated using the discretized operator $\mathbb{L}$ is*

$$\mathcal{E}^{\mathbb{L}} = \langle \phi - \mu^{x(\cdot)}, \eta(\mathbb{L})(\phi - \mu^{x(\cdot)})\rangle. \tag{9}$$

Theorem 1. *The ergodic metric computed using the discrete operator $\mathbb{L}$ converges to the continuous metric computed using Δ as the mesh $\mathscr{M}$ approach W.*

Ergodicity over Meshes. In Eq. (10), we approximate the inner products of arbitrary functions $\mathcal{F}$ with the basis functions $\mathcal{F}_s$. Since the integral over W defines an inner product space, the integral can be discretized over the mesh $\mathscr{M}$ with a mass matrix M, also provided by Sharp and Crane (2020):

$$\int_W \mathcal{F}(w)\mathcal{F}_s(w)\, dw \approx ([\mathcal{F}(w_b)]_{b=1}^{m})^{\top} M \boldsymbol{\mathcal{F}}_s. \tag{10}$$

Thus, we can approximately evaluate the integrals in Eq. (4) and Eq. (5) using the eigenvectors $\boldsymbol{\mathcal{F}}_s$ of $\mathbb{L}$. Thus, the MAS ergodic trajectory optimization over meshable surfaces (Dong et al., 2025) becomes:

$$\begin{aligned} \min_{x(t),u(t)} \quad & \mathcal{E}^{\mathbb{L}}(x(t),\phi) \\ \text{s.t.} \quad & \dot{x}_i = \mathscr{F}_i(x_i(t), u_i(t)), \qquad \forall i \in \{1,\ldots,N\}, \\ & x_i(t) \in X_i,\ u_i(t) \in U_i, \qquad \forall i \in \{1,\ldots,N\}, \end{aligned} \tag{11}$$

where $\mathscr{F}_i : X_i \times U_i \to X_i$ is the agents dynamics.

2.6 Problem Statement

We consider single-integrator dynamics:

$$\dot{x}_i = u_i, \qquad \forall i \in V := \{1,\ldots,N\}. \tag{12}$$

To ensure collision avoidance, a minimum safety distance $d_{\min} > 0$ is enforced as $\|x_j(t) - x_i(t)\| \geq d_{\min}, \quad \forall\, i \neq j.$

Each agent has a limited communication range d_{comm}, inducing a time-varying interaction graph

$$\mathcal{G}(t) = (V, E(t)), \tag{13}$$

where $(i,j) \in E(t)$ if and only if $\|x_i(t) - x_j(t)\| \leq d_{\text{comm}} \wedge \text{LOS}(i,j,t) = 1$, with $\text{LOS}(i,j,t) = 1$ indicating unobstructed LOS. The neighbor set of agent i is $\mathcal{N}_i(t) = \{j \in V \setminus \{i\} \mid (i,j) \in E(t)\}$. We assume $\mathcal{G}(0)$ is connected and enforce connectivity preservation for all $t > 0$, ensuring continuous information flow. A minimum surface clearance $d_{\text{surf}} > 0$ is also imposed, requiring each agent to maintain a safe distance from the target surface. These requirements are enforced through the set of CBFs introduced later in (15)–(18). we define the main problem of this study as follows.

Problem 1. *Consider N agents inspecting a complex non-Euclidean surface represented by a triangular mesh $W \subset \mathbb{R}^3$, which defines the ergodic domain with target density ϕ. Each agent follows single-integrator dynamics (12), where $x_i \in X_i \subset \mathbb{R}^3$ and $u_i \in U_i \subset \mathbb{R}^3$. Design a distributed control input u_i such that all agents follow ergodic trajectories over the surface, minimizing the surface ergodic metric while ensuring collision avoidance, connectivity maintenance, LOS preservation, and safe surface clearance.*

3. SAFE CONNECTED MULTI-AGENT ERGODIC COVERAGE CONTROL

Given Problem 1, we develop a cooperative control framework formulated as a CBF-based quadratic program (CBF-QP) that integrates the surface-ergodic exploration objective in (11) with safety-critical constraints enforced through the CBF formulations introduced in Subsection 2.3. In particular, the pairwise CBF h_{ij}^{mode} encodes the inter-agent constraints, including collision avoidance, distance-based connectivity maintenance, and LOS-based connectivity preservation, whereas the agent-wise CBF h_i^{surf} enforces safe surface clearance with respect to the target surface. The resulting CBF-QP is given by:

$$\min_{x(t),\,u(t)} \quad \mathcal{E}^{\mathbb{L}}(x(t),\phi) + \|u(t) - u^{\text{nom}}(t)\|^2 \tag{14a}$$

$$\text{s.t. } \dot{x}_i(t) = u_i(t),\ x_i(t) \in X_i,\ u_i(t) \in U_i, \quad \forall i \in V, \tag{14b}$$

$$\nabla_{x_i} h_{ij}^{\text{mode}}(x_i,x_j)\cdot u_i(t) + \nabla_{x_j} h_{ij}^{\text{mode}}(x_i,x_j)\cdot u_j(t) \geq -\gamma_{ij} h_{ij}^{\text{mode}}(x_i,x_j), \quad \forall (i,j) \in E, \tag{14c}$$

$$\nabla_{x_i} h_i^{\text{surf}}(x_i)\cdot u_i(t) \geq -\gamma_i^{\text{surf}}\left(h_i^{\text{surf}}(x_i)\right), \forall i \in V. \tag{14d}$$

The nominal control input is defined as an ergodic exploration controller $u_i^{\text{nom}} = k_{\text{erg}} g_i$, where g_i is a weighted exploration direction derived from the mismatch between the desired and empirical visitation distributions, driving agents toward under-explored regions while remaining tangent to the surface, and $k_{\text{erg}} > 0$ is the ergodic gain.

3.1 Joint CBF on Inter-Agent Safety and Connectivity

Since enforcing collision avoidance and connectivity constraints for all agent pairs is computationally expensive, we restrict, for each agent i, the CBF constraints to neighboring agents within an interaction radius $d_{\text{safe}} > d_{\min}$. The corresponding neighbor set is defined as $\mathcal{N}_i^{\text{safe}}(t) = \{j \neq i \mid \|x_j(t) - x_i(t)\| \leq d_{\text{safe}}\}$. For each agent i, and for all neighboring agents $j \in \mathcal{N}_i^{\text{safe}}$, we define the safety CBF

$$h_{ij}^{\text{safe}}(x_i,x_j) = \|x_i - x_j\|^2 - d_{\min}^2, \qquad h_{ij}^{\text{safe}} \geq 0, \tag{15}$$

which ensures that each relevant neighboring pair of agents maintains the minimum safety distance $d_{\min}$.

Similarly, for connectivity maintenance, we consider only agents in the spanning tree introduced in Subsection 2.2, constructed from the communication graph (13) using the communication radius d_{comm}. Preserving these links is sufficient to maintain network connectivity. Accordingly, the connectivity-neighbor set is defined as $\mathcal{N}_i^{\text{conn}}(t) = \{j \in V \setminus \{i\} \mid (i,j) \in E_{\mathcal{T}}(t)\}$, i.e., agents connected to i via the spanning tree $\mathcal{T}(t)$. For all $j \in \mathcal{N}_i^{\text{conn}}(t)$, define

$$h_{ij}^{\text{conn}}(x_i,x_j) = d_{\text{comm}}^2 - \|x_i - x_j\|^2, \quad h_{ij}^{\text{conn}} \geq 0, \tag{16}$$

where $d_{\text{comm}} > 0$ denotes the communication range. CBFs (15)–(16) enforce collision avoidance and connectivity using only local neighbors.

3.2 Line-of-Sight (LOS) Communication Safety

For each tree edge $(i,j) \in E_{\mathcal{T}}$, consider the line segment $s_{ij}(\lambda) = x_i + \lambda(x_j - x_i), \lambda \in [0,1]$, where $x_i, x_j \in \mathbb{R}^n$ denote the positions of agents i and j. The *shortest (Euclidean) distance* between a point $p \in \mathbb{R}^n$ and the unsafe region $X_u^{LOS} \subset \mathbb{R}^n$ is defined as $\text{sdist}(p, X_u^{LOS}) := \inf_{q \in X_u^{LOS}} \|p - q\|$, which satisfies $\text{sdist}(p, X_u^{LOS}) = 0$ if and only if $p \in X_u^{LOS}$. Given a safety margin $d_{LOS} > 0$, the edge LOS-safety barrier function is defined as

$$h_{ij}^{\text{LOS}}(x_i,x_j) = \min_{\lambda \in [0,1]} \text{sdist}^2(s_{ij}(\lambda), X_u^{LOS}) - d_{LOS}^2. \tag{17}$$

3.3 Surface Avoidance

For each agent i, consider its position $x_i \in \mathbb{R}^n$ and the target surface, modeled as a triangular mesh. Let $x_{\text{closest}}(x_i) := \arg\min_{p \in X_u^{\text{surf}}} \|x_i - p\|$ denote the closest point on the unsafe region X_u^{surf} (the target surface). The corresponding distance to the surface is $\text{sdist}(x_i, X_u^{\text{surf}}) = \|x_i - x_{\text{closest}}(x_i)\|$. Then surface-safety CBF is defined as

$$h_i^{\text{surf}}(x_i) = \text{sdist}^2(x_i, X_u^{\text{surf}}) - d_{\text{surf}}^2 \geq 0, \tag{18}$$

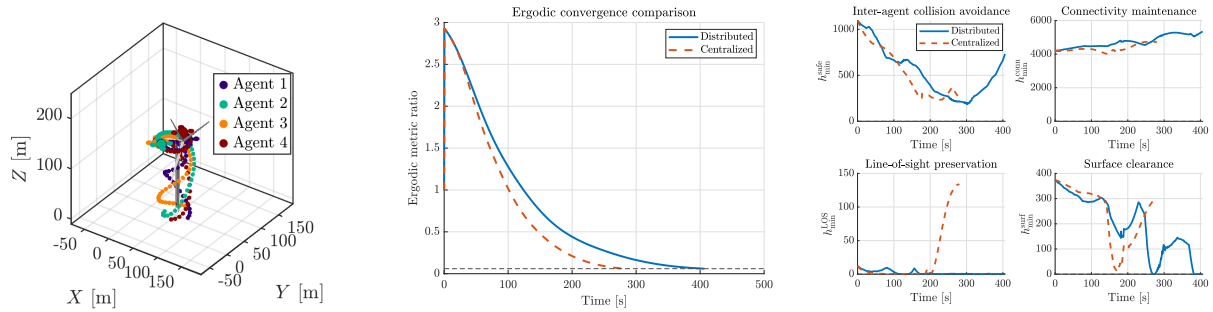
where d_{surf} specifies the minimum required clearance between each agent and the target surface.

3.4 Distributed Control Barrier Function

Enforcing (14c) for the CBFs (15)-(17) requires agent i to incorporate information about agent j. However, since agent i cannot control u_j, we employ a distributed CBF formulation. Let $\mathcal{N}_i^{mode}$ denote the relevant neighbor set associated with the corresponding pairwise barrier function, e.g., N_i^{safe} for collision avoidance and N_i^{conn} for connectivity and LOS preservation. For any pair (i,j), we define a differentiable barrier function $h_{ij}(x_i,x_j)$ whose nonnegativity characterizes admissible states. Under the agent dynamics in (12), the distributed CBF constraint for agent i becomes:

$$\nabla_{x_i} h_{ij}(x_i,x_j)\cdot u_i(t) \geq -\gamma_{ij}\, h_{ij}(x_i,x_j), \quad \forall j \in \mathcal{N}_i^{mode},$$

where $\gamma_{ij} > 0$ is a class-$\mathcal{K}$ gain. Given this constraint, each agent computes an admissible control input by solving the local CBF-QP $u_i^* = \arg\min_{u_i} \|u_i - u_i^{nom}\|^2$ subject to $\nabla_{x_i} h_{ij}(x_i,x_j)\cdot u_i(t) \geq -\gamma_{ij}\, h_{ij}(x_i,x_j),\ \forall j \in \mathcal{N}_i^{mode}$, which minimizes the deviation from the nominal control input while satisfying the safety constraints with respect to neighboring agents. Surface-avoidance constraints (18) for enforces constraint (14d) are agent-wise and do not require



(a) (b) (c)

Fig. 1. (a) Four-agent trajectories around a turbine, (b) ergodic metric convergence, and (c) CBF performance.

a neighbor set. Since each agent enforces constraints (15)-(17) only over local neighbors, the resulting CBF–QP is low-dimensional and solved independently onboard. When enforced by all agents, these distributed conditions collectively maintain the pairwise safety constraints and keep the MAS within the admissible safe set.

3.5 Distributed Ergodic Metric Computation

The classical ergodic metric (Section 2.4) is $\mathcal{E}(x,\phi) = \sum_s \Lambda_s(\mu_s-\phi_s)^2$, where μ_s and ϕ_s are defined in (4)–(5). In the mesh-based setting, the surface ergodic metric is given by (9), equivalently $\mathcal{E}^{\mathbb{L}}(x,\phi) = \langle \phi-\mu^x, \eta(\mathbb{L})(\phi-\mu^x)\rangle = \sum_s \eta(\lambda_s)(\mu_s-\phi_s)^2$, where $\eta(\lambda_s)$ is the spectral weighting function (see Dong et al., 2025 for details). When W is approximated by a triangular mesh $\mathscr{M}$ with vertices $\{w_i\}_{i=1}^m$, the coefficients are computed using the mass matrix M via (10), yielding $\mu_s \approx {\mu^x}^\top M\boldsymbol{\mathcal{F}}_s$, $\phi_s \approx \phi^\top M\boldsymbol{\mathcal{F}}_s$, with $\phi^\top = [\phi(w_1),\cdots,\phi(w_m)]$ and ${\mu^x}^\top = [\mu^x(w_1),\cdots,\mu^x(w_m)]$. In (11), $\mathcal{E}^{\mathbb{L}}(x(t),\phi)$ implicitly incorporates these approximations, so μ_s and ϕ_s are not written explicitly. Although (14) is centralized, distributed computation follows:

Global Ergodic Metric. The global *surface ergodic* metric is defined as $\mathcal{E}^{\mathbb{L}}(x(t),\phi) = \sum_s \eta(\lambda_s)(\mu_s-\phi_s)^2$, where μ_s is the global coefficient $\mu_s = \frac{1}{N}\sum_{i=1}^N \mu_{s,i}$. Each agent i can compute only its local contribution $\mu_{s,i} \approx {\mu_i^{x_i}}^\top M\boldsymbol{F}_s$. No single agent knows all $\mu_{s,j}$ for $j \neq i$, so the global μ_s cannot be computed directly.

Consensus (estimating the global μ_s). Each agent i maintains a local estimate $\hat{\mu}_{s,i}(t) \approx \mu_s$, and updates it by averaging with neighbors:

$$\dot{\hat{\mu}}_{s,i}(t) = \alpha \sum_{j\in N_i} a_{ij}\big(\hat{\mu}_{s,j}(t) - \hat{\mu}_{s,i}(t)\big), \tag{19}$$

where $\alpha > 0$ is a small consensus gain and a_{ij} are the edge weights. Initially, $\hat{\mu}_{s,i}(0) = \mu_{s,i}(0)$. Over time, all $\hat{\mu}_{s,i}(t)$ converge to μ_s through neighbor exchanges, yielding $\hat{\mu}_{s,1} = \cdots = \hat{\mu}_{s,N} = \mu_s$.

Local Ergodic Cost per Agent. Each agent can compute its own ergodic cost locally as $\mathcal{E}_i^{\mathbb{L}}(x_i,\hat{\mu}_{s,i},\phi) = \sum_s \eta(\lambda_s)(\hat{\mu}_{s,i}-\phi_s)^2$. After convergence, $\hat{\mu}_{s,i} = \mu_s$. Thus, each agent effectively computes the global ergodic metric using its local estimate, eliminating the need for a central coordinator. Then, the optimization problem in Eq. (14) is rewritten for all $i \in \{1,\ldots,N\}$ to incorporate CBF constraints for LOS preservation as in (17) and surface avoidance as in (18), while enabling distributed execution. Consequently, the optimization problem that each agent must solve is given by:

$$\begin{aligned}
&\min_{x_i(t),u_i(t)} \quad \mathcal{E}_i^{\mathbb{L}}(x_i,\hat{\mu}_{s,i},\phi) + \|u_i(t) - u_i^{nom}(t)\|^2 \\
&\text{s.t. } \dot{x}_i(t) = u_i(t), x_i(t) \in X_i, u_i(t) \in U_i, \\
&\nabla_{x_i} h_{ij}^{\text{safe}}(x_i,x_j)\cdot u_i(t) \geq -\gamma_{ij}^{\text{safe}}(h_{ij}^{\text{safe}}(x_i,x_j)), \quad \forall j \in \mathcal{N}_i^{\text{safe}}, \\
&\nabla_{x_i} h_{ij}^{\text{conn}}(x_i,x_j)\cdot u_i(t) \geq -\gamma_{ij}^{\text{conn}}(h_{ij}^{\text{conn}}(x_i,x_j)), \forall j \in \mathcal{N}_i^{\text{conn}}, \\
&\nabla_{x_i} h_{ij}^{LOS}(x_i,x_j)\cdot u_i(t) \geq -\gamma_{ij}^{LOS}(h_{ij}^{LOS}(x_i,x_j)), \forall j \in \mathcal{N}_i^{\text{conn}}, \\
&\nabla_{x_i} h_i^{\text{surf}}(x_i)\cdot u_i(t) \geq -\gamma_i^{\text{surf}}(h_i^{\text{surf}}(x_i)).
\end{aligned} \tag{20}$$

4. CASE STUDY

We evaluate the distributed ergodic controller and the CBF-QP formulation (20) on a 3D inspection task involving utility-scale wind turbines composed of a tower, nacelle, and three blades. Each turbine follows V150-scale dimensions and is represented using a triangular surface mesh, with blades modeled as 3D NACA 4412 airfoils. A normalized inspection density ϕ is defined over the mesh, emphasizing the upper tower through a cubic height profile, blade tips through radial weighting from the hub, and the nacelle with a uniform weight. The simulation shown in Fig. 1 considers a single turbine and a team of 4 agents governed by the dynamics (12). At each timestep, agents compute local visitation densities via Gaussian kernel smoothing, project them onto the LB basis, and exchange information over a connected communication graph through distributed consensus. Each agent evaluates its ergodic mismatch and the smoothed spatial gradient $\mathbb{S}^{x_i}(w) = \exp\!\Big(-\frac{\|w-x_i\|^2}{2\sigma^2}\Big)$ defining the sensing footprint. The consensus gain is $\alpha = 0.02$, and the nominal control is filtered through the CBF-QP (20), enforcing safety, connectivity, LOS, and surface constraints (15)–(18) with $d_{\min} = 5\,\text{m}$, $d_{\text{comm}} = 80\,\text{m}$, $d_{\text{LOS}} = 1\,\text{m}$, and $d_{\text{surf}} = 5\,\text{m}$. The trajectories in Fig. 1(a) illustrate the multi-agent inspection behavior around the turbine, while Fig. 1(b)–(c) compares the ergodic convergence and CBF performance of the distributed and centralized controllers, highlighting the tradeoff between coverage efficiency, safety preservation, and computational scalability. Since each agent computes its control action using local consensus-based ergodic estimates and a low-dimensional neighbor-based CBF-QP, the resulting distributed controller remains decentralized, scalable, and real-time implementable, while generating smoother, more spatially separated trajectories with improved inter-agent separation, connectivity main-

Table 1. CBF-QP scalability for four turbines (Cent: centralized, Dist: distributed).

N	QP time [s]		RT success [%]		Constraints	
	Cent	Dist	Cent	Dist	Cent	Dist/agent
16	0.02	0.01	100	100	180	∼10
24	0.10	0.015	100	100	350	∼12
32	0.50	0.02	40	100	600	∼15
48	5.20	0.025	0	100	1300	∼18

tenance, and LOS preservation throughout the mission. In contrast, the centralized controller uses global ergodic information and joint optimization to achieve faster ergodic convergence by aggressively steering agents toward high-priority regions, at the cost of operating closer to safety boundaries, weaker connectivity preservation, and significantly higher computational complexity as the number of agents increases. To evaluate scalability and real-time (RT) feasibility, we consider a four-turbine wind farm with varying numbers of agents, as summarized in Table 1, which reports the average per-step QP solve time for the global centralized QP and the maximum local distributed QP across agents. As the number of agents increases, the centralized QP solve time grows from ~ 0.02 s to over 33 s, while the distributed approach remains nearly constant at 0.01–0.03 s. With RT feasibility defined as $T_{\mathrm{QP}} \leq dt = 0.5$ s, the centralized RT success rate drops from 100% to 0%, whereas the distributed method maintains 100% RT feasibility due to its bounded local constraints per agent, unlike the approximately quadratic scaling of the centralized formulation. Simulations were performed on an Intel i5 3.6,GHz CPU with 16,GB RAM.

5. CONCLUSION

We presented a framework for safe multi-agent ergodic coverage over complex 3D surfaces, combining distributed ergodic optimization with CBF-based safety and connectivity guarantees, and validated it in a wind turbine inspection scenario. LB eigenfunctions enable ergodic search on arbitrary meshes, while CBFs enforce inter-agent safety, distance- and LOS-based connectivity, and collision avoidance. A distributed consensus scheme improves scalability and preserves real-time feasibility in large-scale systems by eliminating centralized computation, while achieving performance comparable to the centralized approach. Future work includes orientation-aware sensing, dynamic environments with moving blades and time-varying ergodic surfaces, robust CBF design under wind disturbances, and relaxing ideal consensus assumptions.

REFERENCES

Ames, A.D., Coogan, S., Egerstedt, M., Notomista, G., Sreenath, K., and Tabuada, P. (2019). Control barrier functions: Theory and applications. In *2019 18th European control conference (ECC)*, 3420–3431. IEEE.

Aminzadeh, A. and Khoshnood, A.M. (2023). Multi-uav cooperative search and coverage control in post-disaster assessment: Experimental implementation. *Intelligent Service Robotics*, 16(4), 415–430.

Borrmann, U., Wang, L., Ames, A.D., and Egerstedt, M. (2015). Control barrier certificates for safe swarm behavior. *IFAC-PapersOnLine*, 48(27), 68–73.

Dong, D., Xu, A., Gutow, G., Choset, H., and Abraham, I. (2025). Ergodic exploration over meshable surfaces. In *2025 IEEE International Conference on Robotics and Automation (ICRA)*, 13088–13094. IEEE.

Egerstedt, M. (2021). *Robot ecology: constraint-based design for long-duration autonomy*. Princeton University Press.

Hildebrandt, K., Polthier, K., and Wardetzky, M. (2006). On the convergence of metric and geometric properties of polyhedral surfaces. *Geometriae dedicata*, 123(1), 89–112.

Ibuki, T., Hirano, T., Funada, R., and Sampei, M. (2023). Optimization-based distributed safety control with applications to collision avoidance for mobile robotic networks. *Advanced Robotics*, 37(1-2), 87–98.

Ivić, S., Crnković, B., Grbčić, L., and Matleković, L. (2023). Multi-uav trajectory planning for 3d visual inspection of complex structures. *Automation in Construction*, 147, 104709.

Kosonen, P., Fadaeian, Y., Eura, R.M., Sulameri, J., Fikri, M.R., and Gusrialdi, A. (2025). Human-drone swarm interaction system for persistent monitoring of large disperse area. In *2025 IEEE 21st International Conference on Automation Science and Engineering (CASE)*, 179–184. IEEE.

Lerch, C., Dong, D., and Abraham, I. (2023). Safety-critical ergodic exploration in cluttered environments via control barrier functions. In *2023 IEEE International Conference on Robotics and Automation (ICRA)*, 10205–10211. IEEE.

Mathew, G. and Mezić, I. (2011). Metrics for ergodicity and design of ergodic dynamics for multi-agent systems. *Physica D: Nonlinear Phenomena*, 240(4-5), 432–442.

Mavrommati, A., Tzorakoleftherakis, E., Abraham, I., and Murphey, T.D. (2017). Real-time area coverage and target localization using receding-horizon ergodic exploration. *IEEE Transactions on Robotics*, 34(1), 62–80.

Miller, L.M. and Murphey, T.D. (2013). Trajectory optimization for continuous ergodic exploration on the motion group SE (2). In *52nd IEEE Conference on Decision and Control*, 4517–4522. IEEE.

Miller, L.M., Silverman, Y., MacIver, M.A., and Murphey, T.D. (2015). Ergodic exploration of distributed information. *IEEE Transactions on Robotics*, 32(1), 36–52.

Rinaldi, G., Thies, P.R., and Johanning, L. (2021). Current status and future trends in the operation and maintenance of offshore wind turbines: A review. *Energies*, 14(9), 2484.

Scott, S.E., Redd, T.C., Kuznetsov, L., Mezić, I., and Jones, C.K. (2009). Capturing deviation from ergodicity at different scales. *Physica D: Nonlinear Phenomena*, 238(16), 1668–1679.

Sharp, N. and Crane, K. (2020). A laplacian for nonmanifold triangle meshes. In *Computer Graphics Forum*, volume 39, 69–80. Wiley Online Library.

Shetty, S., Silvério, J., and Calinon, S. (2021). Ergodic exploration using tensor train: Applications in insertion tasks. *IEEE Transactions on Robotics*, 38(2), 906–921.

Sun, M.M., Gaggar, A., Trautman, P., and Murphey, T. (2025). Fast ergodic search with kernel functions. *IEEE Transactions on Robotics*.

Yang, Y., Lyu, Y., Zhang, Y., Yi, S., and Luo, W. (2024). Decentralized multi-robot line-of-sight connectivity maintenance under uncertainty. *arXiv:2406.12802*.